Mathematical Modelling and Analysis
Volume 5, 2000, pages 32–43

MODELING OF GENERATION DYNAMICS OF PASSIVELY AND ACTIVELY Q-SWITCHED SOLID-STATE LASERS

A. DEMENT'EV[1], R. NAVAKAS[2], R. VAICEKAUSKAS[3]

[1] *Institute of Physics*
Savanorių 231, LT-2028, Vilnius, Lithuania
[2] *Vytautas Magnus University*
Vileikos 8, LT-3035, Kaunas, Lithuania
Vilnius University
Naugarduko 24, LT-2600, Vilnius, Lithuania
E-mail: [1] aldement@ktl.mii.lt, [2]Robertas_Navakas@fc.vdu.lt
E-mail: [3]Rimantas.Vaicekauskas@maf.vu.lt

Received October 5, 1999

ABSTRACT

A theoretical model for simulation of generation dynamics of microchip lasers is presented. A number of physical effects influencing generation of microchip lasers that are usually omitted are accounted. Results of theoretical calculations are in good agreement with experimental data.

1. INTRODUCTION

Solid state microchip lasers with diode pumping are widely used in areas where high power giant pulses are required [1]. Passively Q-switched microchip lasers can produce pulses whose duration is hundreds of picoseconds and repetition rates are tens of kilohertz [1; 2]. Passive Q-switching is achieved using crystalline saturable absorbers, e.g. Cr^{4+} : YAG, Cr^{4+} : GSGG etc. Passive Q-switching permits efficient selection of transversal and longitudinal modes, while active Q-switching enables synchronization of pulse generation times with other processes and reduces timing jitter and fluctuations of intensity and duration of generated pulses. Hybrid passive and active Q-switching

combines advantages of both methods.

Recently, a number of experimental results have been published [3] - [8], however, these papers lack a comparison with a comprehensive theoretical model that would describe generation dynamics of such lasers in a realistic manner. Majority of models used for these purposes are applicable mainly for the bulk lasers and permit simulation of a single giant pulse only. In order to optimize parameters of continuously pumped microchip lasers, it is necessary to simulate entire process of pulse development from the level of quantum fluctuations. Duration of this pulse development process is by several orders of magnitude longer than the duration of the pulse itself.

2. MODELLING OF TRANSMISSION OF $CR^{4+}:YAG$ AND $CR^{4+}:GSGG$ SATURABLE ABSORBERS

Crystalline Cr^{4+} doped absorbers have a number of advantages, including their robustness and optical stability. Main parameters of the Cr^{4+} absorbers are the ground and excited state absorption cross sections σ_0 and σ_e. Various sources list different values of the absorption cross sections [9] - [11]. In order to achieve high transmission by bleaching the saturable absorber efficiently, incident beam should be focused into small spot. Small size of the spot and high intensity of the beam give rise to diffraction and nonlinear processes. Therefore, incident beam undergoes distortions in transverse intensity distribution profile while traversing the absorber. Dependence of transmission curve on the pulse duration has also been reported [11]. In order to determine the absorption cross sections in the Cr^{4+} based saturable absorber considering possible dependence of transmission on incident pulse duration, the five level scheme has been proposed [11]. This scheme includes absorption from two excited state levels, with corresponding absorption cross sections σ_{e1} and σ_{e2}. However, in [11] the transmittivity has been treated in plane wave approximation only and neglecting other nonlinear effects. Therefore, equations for wave intensity could be used. Since in our case the phase characteristics of the pulse are important, equations will be written for slowly varying field amplitude. The complete set of equations governing the propagation of a light pulse in the absorber, taking into account the diffraction, nonlinear Kerr effect and relaxation times for different levels, is the following:

$$\frac{\partial e}{\partial t} + \frac{\partial e}{\partial z} - iD\Delta_r e + \frac{\alpha}{2}e = -\frac{1}{2}[\sigma_0 n_1 + \sigma_{e1} n_2 + \sigma_{e2} n_4]e + i\eta|e|^2 e, \qquad (2.1)$$

$$\frac{\partial n_1}{\partial t} = -\sigma_0 n_1 |e|^2 + \frac{n_2}{\tau_2} + \frac{n_4}{\tau_4}, \qquad (2.2)$$

$$\frac{\partial n_2}{\partial t} = \sigma_0 n_1 |e|^2 - \sigma_{e1} n_2 |e|^2 + \frac{n_3}{\tau_3} - \frac{n_2}{\tau_2} - \frac{n_2}{\tau_{24}}, \qquad (2.3)$$

$$\frac{\partial n_3}{\partial t} = \sigma_{e1} n_2 |e|^2 - \frac{n_3}{\tau_3}, \tag{2.4}$$

$$\frac{\partial n_4}{\partial t} = -\sigma_{e2} n_4 |e|^2 + \frac{n_2}{\tau_{24}} + \frac{n_5}{\tau_5} - \frac{n_4}{\tau_4}, \tag{2.5}$$

$$\frac{\partial n_5}{\partial t} = \sigma_{e2} n_4 |e|^2 - \frac{n_5}{\tau_5}, \tag{2.6}$$

$$n_1 + n_2 + n_3 + n_4 + n_5 = n_0. \tag{2.7}$$

Here $e(r,z,t) = E(r,z,t)/E_0$ is the normalized complex field amplitude, z is longitudinal coordinate normalized to absorber length l_a: $z = z'/l_a$, time $t = t'/t_0$ is normalized to the absorber transit time $t_0 = l_a/v_a$, v_a – light velocity in the absorber, τ_i is the population decay time of i-th level, τ_{ij} – nonradiative transition time from i-th to j-th level, both normalized to t_0. The following notations are used in the above equations: $D = l_a/2k_0 r_0^2$ – the diffraction coefficient, $\Delta_r = \partial^2/\partial r^2 + \partial/r\partial r$ – axially symmetric transverse Laplacian, α – coefficient of nonresonant absorption, $\eta = 2\pi\gamma_2 I_0 l_a/\lambda$ – coefficient of the optical Kerr effect, $I_0 = cnE_0^2/8\pi$ – normalization intensity, c - velocity of light in vacuum, n – refractive index, r_0 – Q-switch radius, n_i – population of i-th level normalized to $\bar{N} = \sigma l_a^{-1}$, where σ is effective cross section of stimulated emission of Nd^{3+}.

Equations (2.1)-(2.7) have been solved using the following initial and boundary conditions:

$$e(r,z,t=0) = 0, n_1(r,z,t=0) = n_0(r,z), n_{2-5}(r,z,t=0) = 0, \tag{2.8}$$

$$e(r,z=0,t) = e_0 f_j(t) \exp[-(r/w_0)^s]. \tag{2.9}$$

Solution of the set of equations (2.1)-(2.9) with corresponding values of σ_0, σ_{e1}, σ_{e2} gives a a value of energy of the pulse exiting the absorber. This way, a transmission curve for saturable absorber (dependence of transmittivity $T = W_{out}/W_{in}$, where $W_{out} = 2\pi \int |e(r,l_a,t)|^2 r dr dt$, $W_{in} = 2\pi \int |e(r,0,t)|^2 r dr dt$, on incident pulse energy) is obtained.

This set of equations has been solved using procedure analogous to that applied for Nd:YAG amplifier [12]. Results of calculation ($\tau_{24} = 30$) suggest that while incident super-Gaussian beam (Fig. 1, curve 1) is distorted significantly at the exit plane (curve 2), the beams with Gaussian intensity distribution along the transverse direction (curve 3) undergo almost no distortions in shape (Fig. 1, curve 4). Calculations analogous to those carried out in [12] have shown that temporally averaged pulse quality factor $M^2(t)$

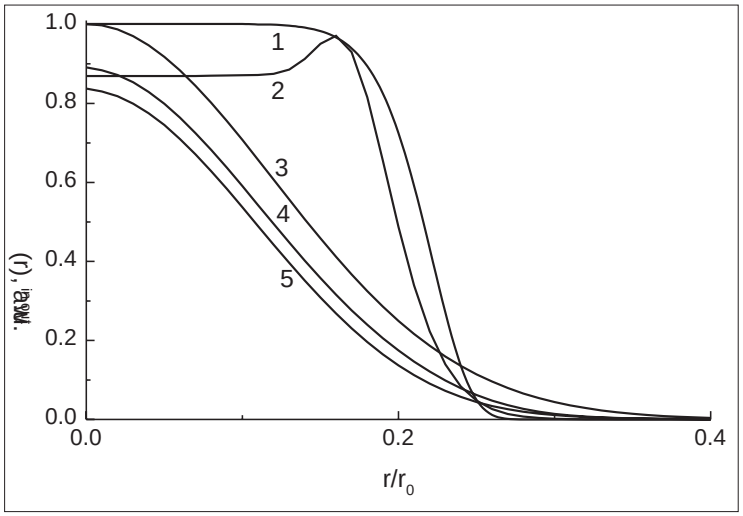

Figure 1. Transverse distribution of incident and absorber transmitted pulses: supergaussian incident beam $s = 10$ (curve 1), Gaussian incident beam $s = 2$ (curve 3), transmitted supergaussian (curve 2) and Gaussian (curve 4) beams. Curves 1 – 4 are obtained for the case of $\tau_{24} = 30$ and curve 5 for $\tau_{24} = 3$.

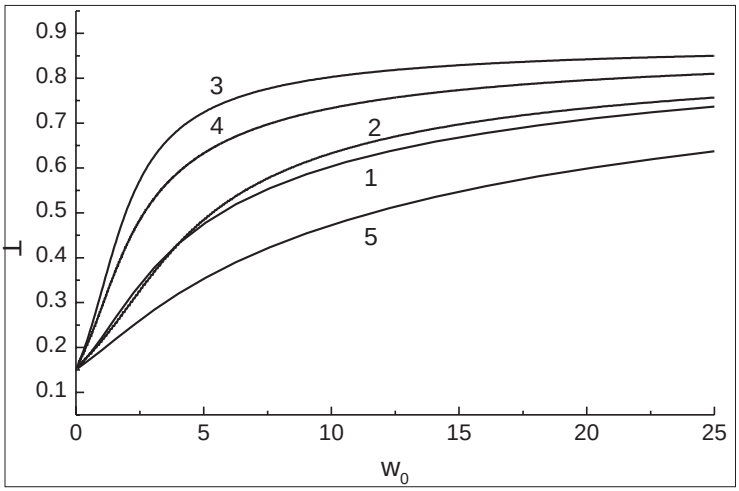

Figure 2. Theoretical transmission curves $T = W_{out}/W_{in}$ of the saturable absorber *vs* energy density W_0 at beam axis calculated using different approximations: five level absorber scheme considering diffraction, $\tau_{24} >> \tau_L$ (curve 1), four level scheme neglecting diffraction, Gaussian beam (curve 2), four level scheme, plane wave approximation (curve 3), four level scheme, plane wave approximation obtained averaging Gaussian intensity distribution (curve 4), five level scheme considering diffraction, $\tau_{24} < \tau_L$ (curve 5).

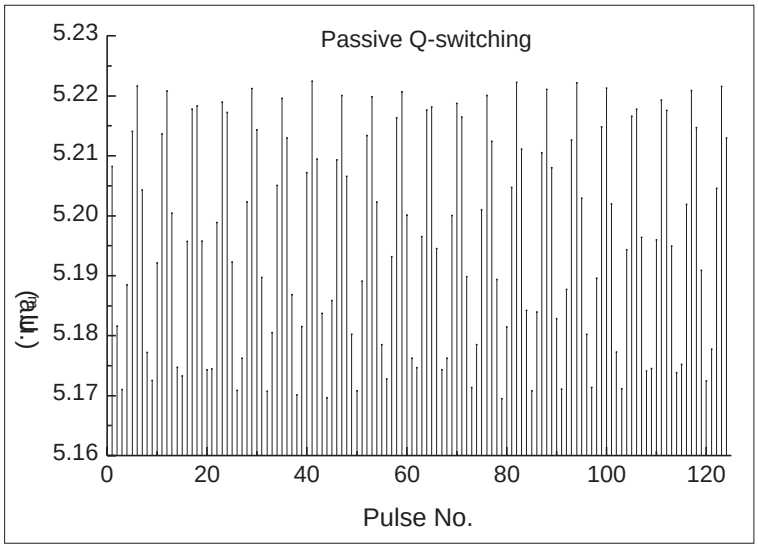

Figure 3. Typical pulse train obtained using microchip laser with passive Q-switching (radiation intensity maximum U_m vs pulse number).

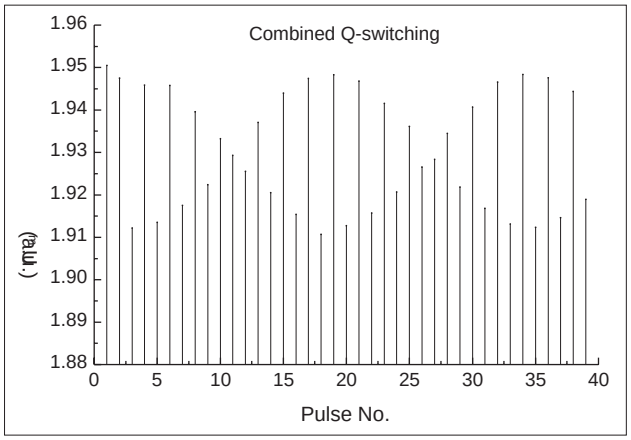

Figure 4. Typical pulse train obtained using microchip laser with combined passive and active Q-switching (radiation intensity maximum U_m vs pulse number).

remains practically unchanged after passage though the absorber even in the saturation regime of absorption of short ($\sim 100ps$) pulses. Theoretical transmission curves calculated using various approximations are given in Fig. 2. It can be seen that for the Gaussian beam transmission curves obtained neglecting diffraction (curve 2) and considering diffraction (curve 1) are pretty close, while plane wave approximation (curve 3) and approximation using averaging of Gaussian beam intensity across the beam axis (curve 4) differ significantly. For the case of slow cross relaxation (curves $1-4$) between singlet and triplet levels ($\tau_{24} = 30$) in comparison to the duration of incident pulse ($\tau_L = 6$) transmission calculated taking into account beam diffraction (curve 1) differs only slightly from the transmission curve calculated using approximation of diffractionless collimated beam (curve 2). This fact substantiates the procedure of determination of the cross sections σ_0 and $\sigma_e \equiv \sigma_{e1}$ using simplified model of the absorber [9]. For the case of short relaxation time $\tau_{24} = 3$ the level 4 is populated effectively. Therefore absorption from two excited levels occurs and the transmission of Q-switch decreases significantly (curve 5). Experimental investigation of transmission dependence on pulse duration in the Nonlinear Optics and Spectroscopy Laboratory of the Institute of Physics has shown no changes for pulse durations ranging from $150ps$ to $2ns$. This result implies that $\tau_{24} >> \tau_L$, and the four level scheme can be used. Note also that in the work [10] it is proposed to use approximation of Gaussian beam with a beam with rectangular intensity distribution (top-hat beam shape). It can be seen that transmission curve for the top-hat beam (curve 3) differs significantly from that for the averaged Gaussian beam (curve 4). It leads to considerable errors while calculating absorption cross sections from experimental data.

3. MODELING OF A Q-SWITCHED SOLID STATE MICROCHIP LASER GENERATION DYNAMICS

In order to develop a comprehensive model for simulation of solid-state microchip laser generation, we start with derivation of corresponding set of equations governing the following processes: temporal variation of field intensity within the cavity, variation of population of lasing levels in active medium and saturable absorber, losses due to active Q-switching of the cavity. Moreover, the model should account for a number of physical effects, such as amplified spontaneous emission in the active medium, finite lifetimes of the upper and lower lasing levels of Nd^{3+}, excited state absorption in the saturable absorber, dependence of absorption cross-sections on orientation of crystallographic axes in respect to polarization of radiation, splitting of lasing levels into sublevels due to Stark effect in the electrical field of crystal lattice, thermalisation times and Boltzmann coefficients of sublevel populations.

The following set of equations describes field intensities I_1 and I_2 for the generated light waves propagating forward and backward within the active medium:

$$\frac{1}{\nu}\frac{\partial I_1}{\partial t'} + \frac{\partial I_1}{\partial z'} = \sigma(f_u N_3 - f_l N_2)I_1 - \alpha I_1, \tag{3.1}$$

$$\frac{1}{\nu}\frac{\partial I_2}{\partial t'} - \frac{\partial I_2}{\partial z'} = \sigma(f_u N_3 - f_l N_2)I_2 - \alpha I_2. \tag{3.2}$$

where ν is the group velocity of light in the active medium, σ is effective cross section at the center of the composite stimulated emission line, $f_u = (\sigma_1 f_{32} + \sigma_2 f_{31})/\sigma$ and $f_l = (\sigma_1 f_{23} + \sigma_2 f_{22})/\sigma$ are effective Boltzman occupation factors for the upper and lower lasing levels, σ_1 and σ_2 - transition cross sections of two overlapping lines constituting the composite contour of the main lasing line at the lasing wavelength which is $\lambda = 1.064\mu m$ in our case. These parameters have the following values at the room temperature [13; 14]: $\sigma = 8.8 \cdot 10^{-19} cm^2$, $\sigma_1 = 7.1 \cdot 10^{-19} cm^2$, $\sigma_2 = 1.9 \cdot 10^{-19} cm^2$, $f_{31} = 0.60$, $f_{32} = 0.40$, $f_{23} = 0.19$, $f_{22} = 0.28$, $f_u = 0.45$, $f_l = 0.21$. α is nonsaturable absorption coefficient.

Set of equations for lasing level populations can be written as follows [14; 15]:

$$\frac{dN_3}{dt'} = R_p(z,t) - \frac{\sigma(I_1 + I_2)}{h\nu}(N_u - N_l) - \frac{N_3}{\tau_{32}}, \tag{3.3}$$

$$\frac{dN_2}{dt'} = \frac{N_3}{\tau_{32}} + \frac{\sigma(I_1 + I_2)}{h\nu}(N_u - N_l) - \frac{N_2}{\tau_{21}}, \tag{3.4}$$

where $R_p(z,t) = w_p(N_1 - N_4)$ is the pumping rate per unit volume, w_p - probability of induced transitions in the pumping channel, τ_{32} and τ_{21} - upper level lifetime and time of radiationless relaxation of the lower lasing level respectively, $h\nu$ - photon energy at the lasing frequency ν, $N_u - N_l = f_u N_3 - f_l N_2$ - effective difference of lasing level populations.

For the purpose of simulation of Q-switched laser the above scheme can be simplified. Since no phase changes in generated pulse shape will be considered, equations for Q-switch can be written for the field intensity instead of equations for field amplitude. The set of equations for the four level passive Q-switch in the simplest case reads as follows [9; 14]:

$$\frac{1}{\nu_a}\frac{\partial I_{a1,2}}{\partial t} \pm \frac{\partial I_{a1,2}}{\partial z} = -\sigma_0 N_{a1} I_{a1,2} - \sigma_e N_{a2} I_{a1,2} - \alpha_a I_{a1,2}, \tag{3.5}$$

$$\frac{\partial N_{a1}}{\partial t} = -\frac{\sigma_0(I_{a1} + I_{a2})}{h\nu} N_{a1} + \frac{N_{a2}}{\tau_{a21}}, \tag{3.6}$$

$$N_{a1} + N_{a2} = N_{a0}. \tag{3.7}$$

Here ν_a is the group velocity of light in the passive Q-switch, σ_0 and σ_e - cross sections of the main and excited state absorption respectively, τ_{a21} - time of radiationless relaxation of the lower excited state level.

Equations (3.1)-(3.7) have been solved in full for the case of single giant pulse generation from the moment when inversion in the active medium reaches its threshold value in the active Q-switch regime [16]. However, for purposes of simulation of the pulse trains exact solution of the set of equations (3.1)-(3.7) with corresponding initial and boundary conditions constitutes a resource-demanding task. It also cannot be used for simulation of short pulse generation from the level of quantum noise, since the pulse duration is smaller by several orders of magnitude than the time of pulse development. Therefore we shall assume the point laser model that is obtained by averaging equations (3.1)-(3.2) along the cavity axis [15]. After averaging and introducing dimensionless variables by normalizing parameters in the equations (3.1)-(3.7), the following set of equations is obtained:

$$\chi\frac{du}{dt} = [n_u - n_l - \sum_i(\sigma'_{0i}n_{a1}^{(i)} + \sigma'_{ei}n_{a2}^{(i)})f_i(\theta)]u - [\alpha + \alpha_a + \alpha_R + \alpha_Q(t)]u + \epsilon\frac{n_3}{\tau_{32}}, \tag{3.8}$$

$$\frac{dn_3}{dt} = \bar{R}_p(t) - u(n_u - n_l) - \frac{n_3}{\tau_{32}}\exp[f_u n_3 l_{ASE}], \tag{3.9}$$

$$\frac{dn_2}{dt} = u(n_u - n_l) + \frac{n_3}{\tau_{32}} - \frac{n_2}{\tau_{21}}, \tag{3.10}$$

$$\frac{dn_{a1}^{(i)}}{dt} = r_p(t) - \beta\bar{\sigma}_0^{(i)}n_{a1}^{(i)}f_i(\theta)u + \frac{n_{a2}^{(i)}}{\tau_{a21}}, \tag{3.11}$$

$$n_1 + n_2 + n_3 = n_0, \tag{3.12}$$

$$n_{a1} + n_{a2} = n_{a0}. \tag{3.13}$$

Relative stuffing of the cavity with active medium and saturable absorber is accounted for by introducing the parameter $\chi = \{l/\nu + l_a/\nu_a + l_e/\nu_e + [L - (l + l_a + l_e)]/c\}/(l/\nu)$, where L is the cavity length, l and l_a - lengths of active

Table 1.
Relative jitter of pulse parameters (Standard deviation.)

	1	2	3	4
$\sigma_n(\Delta)$,	0.0010	0.0010	0.8532	0.0017
$\sigma_n(\mathrm{U_m})$,	0.0198	0.0198	0.3469	0.7134
$\sigma_n(\mathrm{FWHM})$,	0.0203	0.0203	0.2157	0.3317
$\sigma_n(\mathrm{W})$,	0.0172	0.0172	0.1202	0.3880

medium and saturable absorber respectively, l_e and ν_e - effective lengths and group velocity of light in the rest of the elements placed inside the cavity. Other variables are as follows: u - averaged radiation intensity inside the cavity normalized to $I_0 = h\nu/\sigma t_0$, n_i and n_{ai} - occupation densities of levels in the active medium and Q-switch respectively, n_u and n_l - occupation densities of lasing sublevels in the active medium, all normalized to $N = (\sigma l)^{-1}$, α, α_a, α_R, $\alpha_Q(t)$ - dimensionless coefficients of nonsaturable losses, ϵ - coefficient accounting for the fluctuations of number of spontaneous photons in the lasing mode, $\bar{R}_p(t)$ and $r_p(t)$ - normalized rates of pumping in the active medium and pre-lighting of the passive Q-switch, β - ratio of cross sections of the beam in the active medium and passive Q-switch (that can be modified using a telescope inside the cavity), $\sigma'_{0,e} = \sigma_{0,e} l_a/\sigma l$ and $\bar{\sigma}_{0,e}/\sigma$ - effective and relative dimensionless absorption cross sections from the main and excited states of the Q-switch. $f_1(\theta) = \cos^2\theta$, $f_2(\theta) = \sin^2\theta$ are the coefficients accounting for angular dependence of absorption on angle θ between absorber's crystallographic axes and polarization of generated radiation, and σ'_{0i} and σ'_{ei} are the components of absorption cross sections for crystallographic axes oriented in x ($i = 1$) and y ($i = 2$) directions, $n_{ak}^{(i)}$ - populations of the ground ($k = 1$) and excited ($k = 2$) levels with phototropic centers of i-th orientation. For dimensionless relaxation times T'_{ij} normalized to $t_0 = l/\nu$, previous notations are retained for simplicity. Amplified spontaneous emission is accounted for fenomenologically by introducing coefficient l_{ASE} into equation (3.9). Quantum fluctuations are determined by the coefficient ϵ which can be either constant $\epsilon = const$ or fluctuating around some constant background value γ_1: $\epsilon = \gamma_1 - \gamma_2 + 2 \cdot \gamma_2 * \mathrm{rnd}(t)$, where γ_1 is the constant background value, γ_2 is absolute intensity of the fluctuations and $\mathrm{rnd}(t)$ is the random time-dependent value between 0 and 1. Pumping power fluctuations are considered in the same way, by adding a random time-dependent value to the constant value $\bar{R}_p$.

Intensity and energy density of radiation emanating from the cavity are $u_{1,2}(t) = \alpha'_{R_{1,2}} u(t)$ and $w_{1,2} = \int_{t_2}^{t_1} u_{1,2}(t)dt$ respectively, where $\alpha'_{R_{1,2}} = (1 - R_{1,2})/(1 + R_{1,2})$ is intensity loss due to emanation of radiation from the cavity [14; 15].

Active electrooptical Q-switch is simulated by introducing time-dependent loss coefficient $\alpha_Q(t)$:

$$\alpha_Q(t) = \begin{cases} \ln(1/T_1), & 0 \le t \le t_1, \\ \ln(1/T_1) - \frac{t-t_1}{t_2-t_1} \ln(T_2/T_1), & t_1 \le t \le t_2, \\ \ln(1/T_2), & t > t_2. \end{cases} \tag{3.14}$$

here T_1 is the transmittivity of the Q-switch in closed state, T_2 - its transmittivity in open state. It is assumed that the Q-switch is closed ($T = T_1$) till the time t_1, then its transmittivity rises linearly and attains the value T_2 at the time t_2.

The set of equations (3.8)-(3.13) has been solved numerically using the

Dormand- Prince finite difference scheme [17]. Initial conditions assumed were that in the beginning all the Nd^{3+} ions in the active medium and Cr^{4+} ions in the saturable absorber are in the ground state and the calculation starts from the instant when the pumping is switched on. Numerical solution yelds temporal depenedencies of radiation intensity both inside and outside the cavity, as well as the values of populations of levels in the active medium and saturable absorber. Calculation of pulse trains permits to store parameters and generation times of every single pulse for subsequent calculation of statistical parameters of the pulse train, such as timing jitter, deviations of power, energy and duration. Typical pulse trains are shown in Figs. 3, 4. Comparative theoretical results of fluctuations of temporal spacing between pulses, peak intensity, pulse duration and pulse energy for different natures of quantum noise and pumping power and different Q-switching schemes (pasive vs combined) are given in the Table 1, here the first column gives results for stable pumping, constant noise $\Delta R_p = 0$, $\gamma_2 = 0$, the second column gives results for stable pumping, normal noise $\Delta R_p = 0$, $\gamma_2 \neq 0$, the third column – for passive Q-switching, fluctuating pumping and noise $|\Delta R_p|/R_p = 0.01$, $\gamma_2 \neq 0$, the fourth column – for combined Q-switching, fluctuating pumping and noise $|\Delta R_p|/R_p = 0.01$, $\gamma_2 \neq 0$. As it can be seen from the table, here the first column gives results for stable pumping, constant noise Δ application of combined passive and active Q-switching can reduce significantly pulse timing jitter arising from both quantum noise and pumping instabilities.

4. CONCLUSIONS

Calculation results are in good agreement with experimental data reported in [3] -[8] for most of the pulse parameters: pulse shape and duration, repetition rate, energy and power. The model described above allows to calculate timing jitter arising from fluctuations of pumping intensity and spontaneous emission during the period of pulse development from the level of quantum fluctuations. Unfortunately, experimental data about jitter and pumping instabilities is often insufficient to compare it to the theoretical results, but qualitative characteristics of the jitter agree well with those observed experimentally [7]. Specifically, application of combined passive and active Q-switching permits to reduce the timing jitter significantly in comparison to the case of passive Q-switching alone.

R. Navakas thanks Lithuanian State Science and Studies Foundation for support during preparation of this work.

REFERENCES

[1] J. Zayhowski. Q-switched microchip lasers find real-world applications. *Laser Focus World*, **35**, 1999, 129 – 136.

[2] J.J. Zayhowski and J. Harrison. Miniature solid-state lasers. In: *Handbook of photonics*, Mool C. Gupta (Ed.), CRC Press, New York, 1997, 326 – 392.

[3] J.J. Zayhowski and C. Dill . III. Diode-pumped passively Q-switched picosecond microchip lasers. *Opt. Lett.*, **19**, 1994, 1427 – 1429.

[4] I. Freitag, A. Tünnermann and H. Welling. Passively Q-switched Nd:YAG ring lasers with high average output power in single-frequency operation. *Opt. Lett.*, **22**, 1997, 706 – 708.

[5] P.K. Lam, I. Freitag, M. Bode, A. Tünnermann and H. Welling. High average power Q-switched second harmonic generation with diode-pumped Nd:YAG laser. *Electron. Lett.*, **34**, 1998, 666 – 668.

[6] U. Bäder, J. Bartschke, I. Klimov, A. Borsutzky and R. Wallenstein. Optical parametric oscillator of quasi-phasematched $LiNbO_3$ pumped by a compact high repetition rate single-frequency passively Q-switched Nd:YAG laser . *Opt. Commun.*, **147**, 1998, 95 – 98.

[7] B. Hansson, M. Arvidsson, M. Holmgren and C. Lindström. A combined actively and passively Q-switched microchip laser . In: *Advanced Solid-State Lasers - 98*, Technical Digest (OSA, Washington), 1998, 361 – 363.

[8] S. Spiekermann, M. Bode, C. Fallnich, H. Welling and I. Freitag. Actively Q-switched miniature Nd:YAG ring laser in single-frequency operation. *Electron. Lett.*, **43**, 1998, 2246 – 2247.

[9] R. Buzelis, A. Dement'ev, E. Kosenko, E. Murauskas, F. Ivanauskas and M. Radzhiunas. Determination of absorption cross sections of Cr^{4+} : GSGG and Cr^{4+} : YAG passive Q-switches at the generation wavelength of Nd:YAG laser. *Lith. Phys. Journ.*, **37**, 1997, 246 – 252.

[10] Z. Burshtein, P. Blau, Y. Kalisky, Y. Shimony and M.R. Kokta. Excited-state absorption studies of Cr^{4+} ions in several garnet host crystals. *IEEE J. Quantum electron.*, **34**, 1998, 292 – 299.

[11] S.H. Yim, D.R. Lee, B.K. Rhee and D. Kim. Nonlinear absorption of Cr^{4+} : YAG studied with lasers of different pulsewidths. *Appl. Phys. Lett.*, **73**, 1998, 3193 – 3195.

[12] R. Buzelis, A. Dement'ev, J. Kosenko, E. Murauskas, R. Vaicekauskas and F. Ivanauskas. Amplification efficiency and quality alteration of short pulses amplified in the Nd:YAG amplifier in the saturation mode. *Lith. Phys. Journ.*, **38**, 1998, 289 – 301.

[13] G.M. Zverev and Yu.D. Golyaev. *Crystalline lasers and their applications.* Radio i Svyaz, Moscow, 1994. (In Russian)

[14] R. Buzelis, A. Dementjev, J. Kosenko, E. Murauskas, R. Navakas and M. Radzhiunas. Generation of short pulses with low jitter in combined actively and passively Q-switched Nd:YAG laser with short resonator. *Lith. Phys. Journ.*, **38**, 1998, 248 – 257.

[15] A.L. Mikaelyan, M.L. Ter-Mikaelyan and Y.G. Turkov. Solid State Optical Generators. *Sov. Radio,* Moscow, 1967. (In Russian)

[16] R. Buzelis, R. Vaicekauskas, A. Dement'ev, F. Ivanauskas, E. Kosenko, E. Murauskas and M. Radzhiunas. Numerical analysis and experimental investigation of generation, SBS-compression and amplification of short pulses of Nd:YAG laser. *Izvestiya akademii nauk, ser. fiz.*, **60**, 1996, 168 – 177.(In Russian)

[17] E. Hairer, S.P. Nørsett and G. Wanner. *Solving ordinary differential equations. Nonstiff problems.* Mir, Moscow, 1990. (In Russian)

KIETAKŪNIŲ LAZERIŲ SU PASYVIA IR AKTYVIA KOKYBĖS MODULIACIJA GENERACIJOS DINAMIKOS MODELIAVIMAS

A. DEMENT'EV, R. NAVAKAS, R. VAICEKAUSKAS

Kietakūniai lazeriai su pasyvia ir aktyvia kokybės moduliacija naudojami įvairiose mokslo ir technikos srityse. Tarp kietakūnių lazerių plačiausiai naudojami iki šiol yra lazeriai Nd:YAG pagrindu. Pasyvi kokybės moduliacija yra paprasčiausias kokybės moduliacijos būdas. Todėl Cr^{4+} : YAG ir giminingų kristalų įsisotinimo mechanizmai plačiai tyrinėjami. Naudojant keturių lygmenų modelį su greita relaksacija, gautos paprastos analizinės išraiškos įsisotinančiai sugerčiai. Tačiau toks modelis neleidžia įskaityti skirtumo tarp nanosekundinių ir pikosekundinių impulsų, naudojamų eksperimentuose, ir gausinio intensyvumo pasiskirstymo pluošto skerspjūvyje. Šiame darbe siūlomas patobulintas modelis Cr^{4+} : YAG sugerties skerspjūvių nustatymui.

Parodyta, kad turi būti įskaityti šuoliai tarp sužadintų singletinio ir tripletinio lygmenų penkių lygmenų schemoje, siekiant įskaityti skirtingas žadinančių impulsų trukmes. Siūlomo modelio lygtyse atsižvelgta į žadinančio pluošto difrakciją, todėl tinkamai aprašomas sufokusuoto pluošto sklidimas įsisotinančiame sugėriklyje. Skaitmeniniam lygčių sistemos sprendimui naudotas atskyrimo pagal fizikinius daugiklius būdas. Taikytas atskyrimo būdas tenkina tvermės dėsnio diferencialiniam uždaviniui baigtinių skirtumų analogą. Šiame darbe pateiktas sugėriklio modelis įgalina detalų impulsų su sudėtinga erdvine-laikine struktūra pralaidumo dinamikos modeliavimą.

Neseniai pademonstruoti miniatiūriniai mikrolazeriai Nd pagrindu su pasyvia kokybės moduliacija, kurių rezonatoriaus ilgiai yra milimetrų eilės ir kurie kaupinami lazeriniais diodais. Šie įrenginiai generuoja impulsus, kurių pasikartojimo dažniai kilohercų eilės ir kurių trukmės siekia $100ps$. Jų generacija stabilesnė negu daugelio sistemų su modų sinchronizacija. Lazerių su pasyvia kokybės moduliacija trūkumas yra žymi impulso pasirodymo momentų sklaida, veikiant impulsų serijos generacijos režime. Gerai žinoma, kad lazeriai su kombinuota aktyvia ir pasyvia kokybės moduliacija pasižymi žymiai mažesne laikine sklaida. Šiame darbe siūlomas teorinis modelis kieto kūno mikrolazerių su kokybės moduliacija ir nuolatiniu diodiniu kaupinimu generacijos modeliavimui, atsižvelgiant į apatinio darbinio lygmens baigtinę gyvavimo trukmę, sugertį iš sužadintos būsenos įsisotinančiame sugėriklyje, savaiminio spinduliavimo ir kaupinimo energijos fluktuacijas, įsisotinančio kristalinio sugėriklio kristalografinių ašių orientaciją spinduliuotės poliarizacijos atžvilgiu ir pan. Parodyta, kad rezultatai, gauti naudojant šį modelį, gerai sutampa su žinomais eksperimentiniais rezultatais.